

Online Appendix for
Attention in Motion: Using Scroll Tracking to Measure the
Dynamics of Preferential Choice

Ilkka Leppänen

Aalto University

Contents

S1 Deviations from pre-registration	3
S2 Screenshots	4
S2.1 Alternative stimuli	4
S3 Robustness checks	5
S3.1 Fast scrolling and dwell times	5
S3.2 Quick U-turns and switches	5
S3.3 Robustness check results	5
S4 Computational modelling details	8
S4.1 DDM estimation summary tables	9
S4.2 RT distributions	11
S5 Risky choice experiment	14
S5.1 Method	14
S5.2 Results	15
S5.3 Re-analysis of the SK18 data	25
S6 Comparison of response metrics between studies	26

S1 Deviations from pre-registration

Link to consumer choice study registration: <https://doi.org/10.17605/OSF.IO/H3A74>

Link to money-risk study registration: <https://doi.org/10.17605/OSF.IO/7CDBG>

- Instead of using 90 decision rounds, the consumer choice study contained 120 rounds. This increase was introduced after pilot testing and before the main data collection.
- In addition to analysing last scrolls, first scrolls were analysed in the spirit of exploratory analysis; a first scroll was coded as 1 if it was to the left, otherwise it was coded as 0. This analysis paradigm is in line with the literature on the first locations of eye gaze dwells (e.g. Cavanagh et al., 2014).
- Change in robustness check: the pre-registered description of the robustness check on dwell time measurement has changed, see Section S3. As this is a robustness check, the change does not affect the main confirmatory hypothesis testing.

S2 Screenshots

S2.1 Alternative stimuli

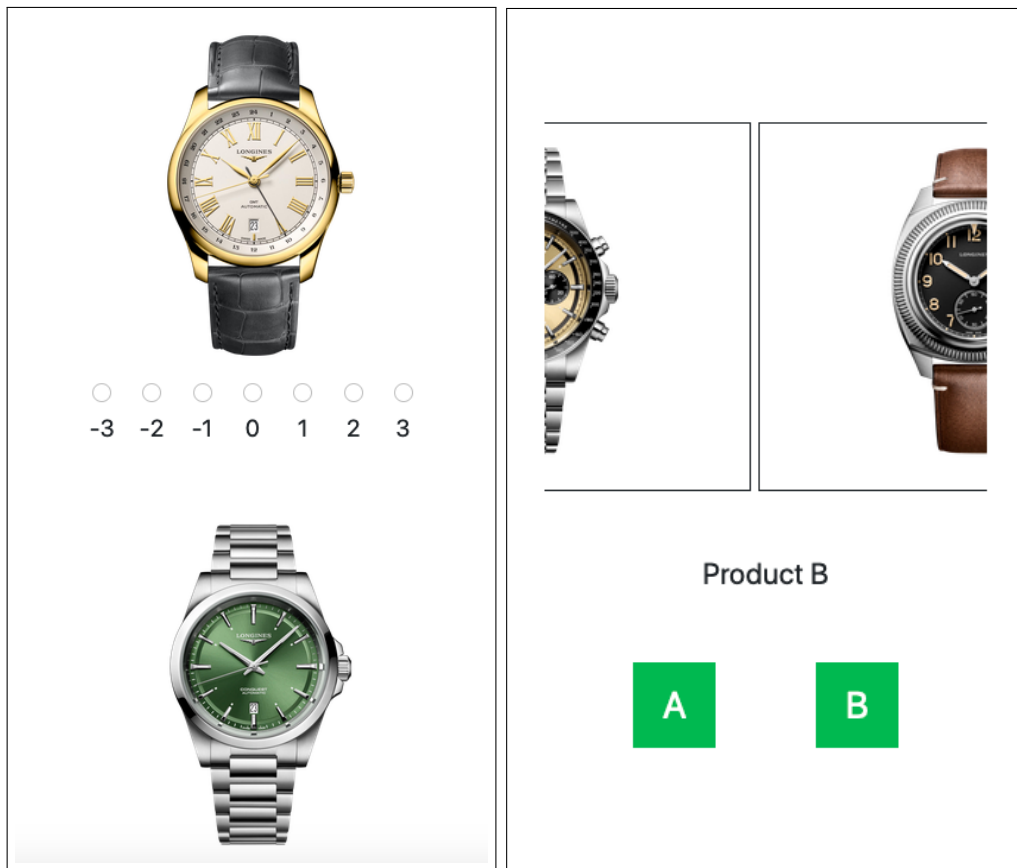


Figure S1: Alternative stimuli, Longines wrist watches, which were shown to 60 subjects, while the other 60 subjects saw Nike trainers as the stimuli (screenshots in the main paper); preference task (left), choice task (right)

S3 Robustness checks

S3.1 Fast scrolling and dwell times

Movement of the scroll bar is typically rapid when shifting from one side to the other, and, during these fast scrolls, the time between successive measurement points is $\ll 100$ ms. One might argue that the $RDV(t)$ signal (see Subsection 1.2 of the main paper) does not change during these fast scroll bar “saccades”. However, the dwell time measurement in the paper considers dwell time to be the total time that the scroll bar spends on either side, including time spent transitioning between sides. Although it is plausible to assume that fast scrolls between options are symmetrically distributed and may not cause a large bias to the results obtained in the study, a robustness check is still required.

Thus, an alternative dwell time metric is defined where such fast scrolls are not counted towards dwell times. See Figure S2 for an illustration. In this alternative metric, all fast scroll bar movements are subtracted from all dwell time measurements used in the main analysis, and the choice-scrolling and value-scrolling link analyses are repeated. Fast scrolling is defined in the following way. As dwell times are a series sum $(t_1 - t_0) + (t_2 - t_1) + \dots$ where each t_i is a y-coordinate (time stamp) in the response curve S , terms $(t_i - t_{i-1}) < 80$ ms are considered fast and consequently excluded. On average, subjects engaged in 942 ms of such fast scrolling during their decision making, from a mean decision time of 2386 ms.

S3.2 Quick U-turns and switches

Some scrolls display quick reversals of scrolling direction, where the option is visible for a short duration only, such that no real information is processed. To investigate the robustness of the switches metric results to such quick U-turns, switches are excluded where the time spent scrolling over an option is less than 500 ms. See Figure S3 for an illustration. Such U-turns are present in 4.5% of all response curves.

S3.3 Robustness check results

Table S1 presents the choice-scrolling re-analysis (Eq. 12 in the main paper) with robust response metrics: β_2 , describing the impact of the proportional scrolling metric on choice, is lower for the

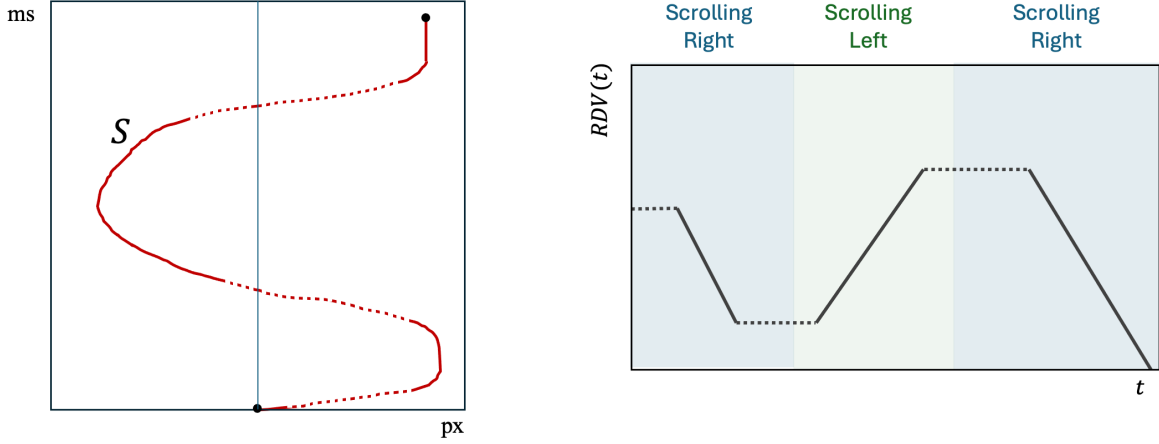


Figure S2: Robustness check on dwell time measurement; the dashed line in the response curve S (left panel) and the $RDV(t)$ signal (right panel) represents fast movement of the scroll bar during which $RDV(t)$ remains constant.

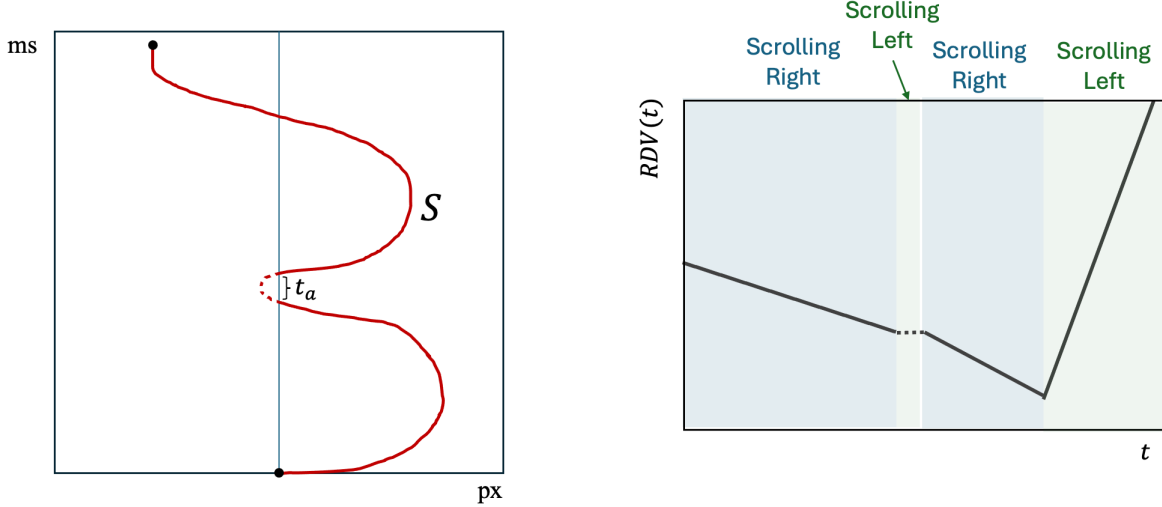


Figure S3: Robustness check on switches measurement; the dashed line in the response curve S (left panel) and the $RDV(t)$ signal (right panel) represents reversal of the scroll bar direction, for the duration t_a , during which $RDV(t)$ remains constant.

DDM with DT and higher for the DDM with W than in the main paper (Table 1). Table S2 presents the value-scrolling re-analysis (Eq. 13) with robust response metrics: again, we see that β_1 , describing the impact of the proportional scrolling metric on subjective value, is lower for the DDM with DT and higher for the DDM with W than in the main paper. These results imply that while the strong-choice scrolling and value-scrolling links are preserved, some of the strength is attributable to the portion of dwell time recorded during fast scrolling. On the other hand,

removing quick U-turn switches strengthens the relationships.

Table S1: Re-investigation with a logit-GLMM of the choice-scrolling link (Eq. 12 in the main paper) with proportional response metrics derived using robust DT and W measurements

	(1)	(2)
β_0	-0.041 [-0.14, 0.058]	-0.017 [-0.18, 0.14]
β_1	1.26 [1.21, 1.31] ***	1.24 [1.19, 1.29] ***
$\beta_2(DT)$	0.95 [0.90, 1.0020] ***	
$\beta_2(W)$		2.031 [1.92, 2.14] ***
RE: subject (SD)	0.50	0.85
Num. obs.	14 200	14 200

Note. RE = random effects, 95% CIs in brackets, significance: *** $p < 0.001$

Table S2: Re-investigation with an LMM of the value-scrolling link predicting V_L when $V_R = 0$, Eq. 13 in the main paper) with proportional response metrics derived using robust DT and W measurements

	(1)	(2)
β_0	-0.12 [-0.35, 0.11]	-0.13 [-0.36, 0.10]
$\beta_1(DT)$	0.47 [0.39, 0.55] ***	
$\beta_1(W)$		0.37 [0.29, 0.45] ***
RE: subject (SD)	1.14	1.15
RE: residual (SD)	1.70	1.72
Num. obs.	2270	2270

Note. RE = random effects, 95% CIs in brackets, significance: *** $p < 0.001$

S4 Computational modelling details

The DDM assumes that observed RTs and choices arise from a diffusion process that is determined by parameters ν , a , z , and t_0 , which are described in the main paper. In all DDMs, the drift rate ν is hierarchical, i.e. modelled as a linear function of an intercept and the predictors, as specified by Eqs. 8 and 9, and random effects that vary across subjects. For example, in the additive model

$$\nu \sim \beta_0 + \beta_1 \Delta V + \beta_2 \Delta \text{PRM}$$

it is assumed that the fixed effect intercept and regressors have normal priors, and the random effects consist of an individual-level offset and a group-level scaling parameter σ_s , where the offset parameter has a standard normal prior and the group-level scaling parameter has a Weibull Beta prior. The other DDMs follow a similar approach in assigning priors for ν . The remaining DDM parameters are assigned weakly informative priors. The non-decision time t_0 and the boundary separation a are assigned half normal priors. The starting point z has explicit bounds in $(0, 1)$ and a uniform prior.

S4.1 DDM estimation summary tables

Table S3 presents a summary of the marginal posterior distributions for the β coefficients of the basic and additive models. Table S4 displays a summary of the marginal posterior distributions for the γ coefficients of the multiplicative models.

Table S3: Marginal posterior summary statistics from the basic and additive models; HDI = highest density interval, ESS = effective sample size

DDM	Parameter	Mean	SD	HDI 2.5%	HDI 97.5%	ESS
Basic	a	1.333	0.007	1.320	1.346	17324
	t_0	0.708	0.005	0.699	0.717	17424
	z	0.502	0.003	0.496	0.509	19443
	σ_s	0.160	0.016	0.128	0.192	4054
	ν coefficients					
	intercept (β_0)	-0.020	0.018	-0.055	0.016	7253
	ΔV (β_1)	0.532	0.008	0.516	0.548	21909
Additive (ψ)	a	1.369	0.007	1.355	1.382	26887
	t_0	0.697	0.005	0.688	0.706	27126
	z	0.503	0.003	0.496	0.509	29589
	σ_s	0.231	0.019	0.196	0.268	5193
	ν coefficients					
	intercept (β_0)	-0.021	0.023	-0.068	0.024	4761
	ΔV (β_1)	0.475	0.008	0.459	0.491	33409
	ΔPRM (β_2)	0.306	0.009	0.288	0.323	26426
Additive (DT)	a	1.376	0.007	1.362	1.390	23550
	t_0	0.695	0.005	0.686	0.705	23873
	z	0.504	0.003	0.497	0.510	26447
	σ_s	0.236	0.019	0.198	0.273	4334
	ν coefficients					
	intercept (β_0)	-0.026	0.024	-0.075	0.019	4443
	ΔV (β_1)	0.469	0.008	0.453	0.485	28058
	ΔPRM (β_2)	0.338	0.009	0.321	0.356	27150
Additive (W)	a	1.399	0.007	1.385	1.414	24804
	t_0	0.689	0.005	0.680	0.699	26013
	z	0.504	0.003	0.498	0.511	31817
	σ_s	0.307	0.023	0.262	0.351	3914
	ν coefficients					
	intercept (β_0)	-0.024	0.031	-0.086	0.035	2285
	ΔV (β_1)	0.443	0.008	0.427	0.459	37369
	ΔPRM (β_2)	0.454	0.011	0.433	0.475	24280

Table S4: Marginal posterior summary statistics from the multiplicative models; The coefficients are denoted as follows: $C_1 \equiv \text{PRM}_L V_L - \text{PRM}_R V_R$, $C_2 \equiv \text{PRM}_R V_L - \text{PRM}_L V_R$; HDI = highest density interval, ESS = effective sample size.

DDM	Parameter	Mean	SD	HDI 2.5%	HDI 97.5%	ESS
Multiplicative (ψ)	a	1.333	0.007	1.321	1.347	20807
	t_0	0.707	0.005	0.698	0.716	20997
	z	0.502	0.003	0.496	0.509	21667
	σ_s	0.158	0.016	0.127	0.190	4286
	ν coefficients					
	intercept (γ_0)	-0.019	0.018	-0.054	0.017	7307
	C_1 (γ_1)	0.342	0.009	0.324	0.360	19977
	C_2 (γ_2)	0.266	0.009	0.248	0.283	19653
Multiplicative (DT)	a	1.333	0.007	1.321	1.347	17705
	t_0	0.707	0.005	0.698	0.716	18687
	z	0.502	0.003	0.496	0.509	19561
	σ_s	0.157	0.016	0.127	0.189	4478
	ν coefficients					
	intercept (γ_0)	-0.020	0.018	-0.055	0.015	7616
	C_1 (γ_1)	0.338	0.010	0.318	0.357	20521
	C_2 (γ_2)	0.257	0.010	0.238	0.276	18846
Multiplicative (W)	a	1.333	0.007	1.320	1.346	21584
	t_0	0.707	0.005	0.698	0.716	20905
	z	0.502	0.003	0.496	0.509	20118
	σ_s	0.159	0.016	0.128	0.191	4531
	ν coefficients					
	intercept (γ_0)	-0.020	0.018	-0.056	0.015	6779
	C_1 (γ_1)	0.316	0.013	0.291	0.340	18990
	C_2 (γ_2)	0.254	0.012	0.230	0.279	19827

S4.2 RT distributions

Figures S4, S5, and S6 show observed RTs and RTs from the posterior predictive distribution, with flipped values for Right choices, separately for each level in value difference ΔV .

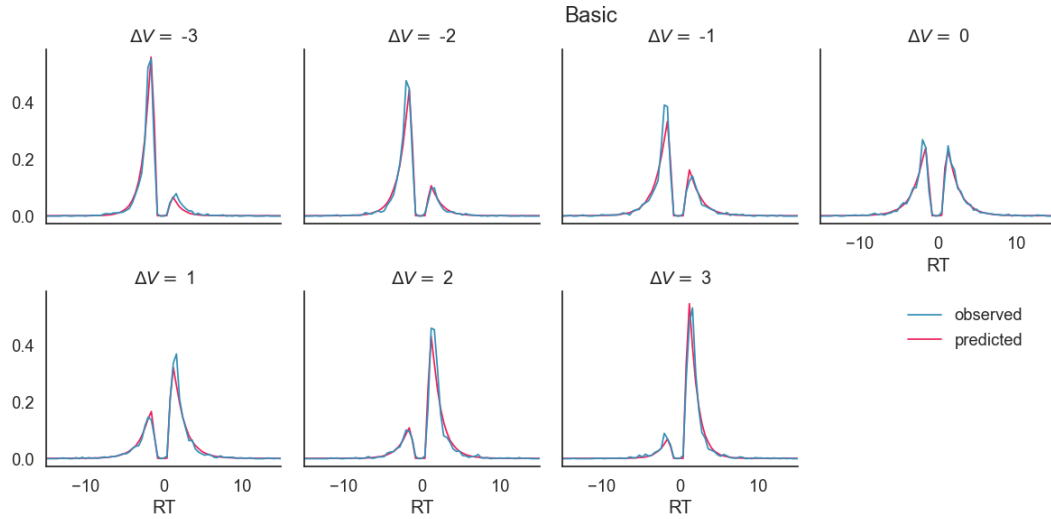


Figure S4: RT distributions (observed and predicted posteriors) from the basic DDM; negative values = Right choices, positive values = Left choices

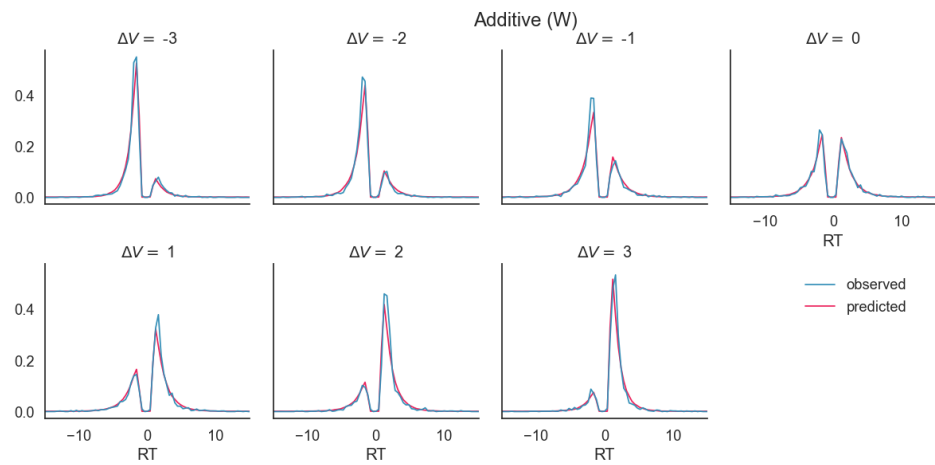
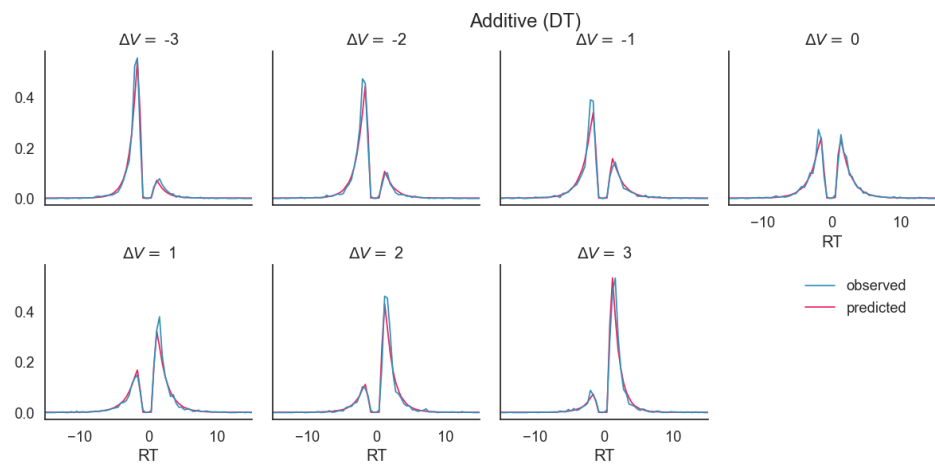
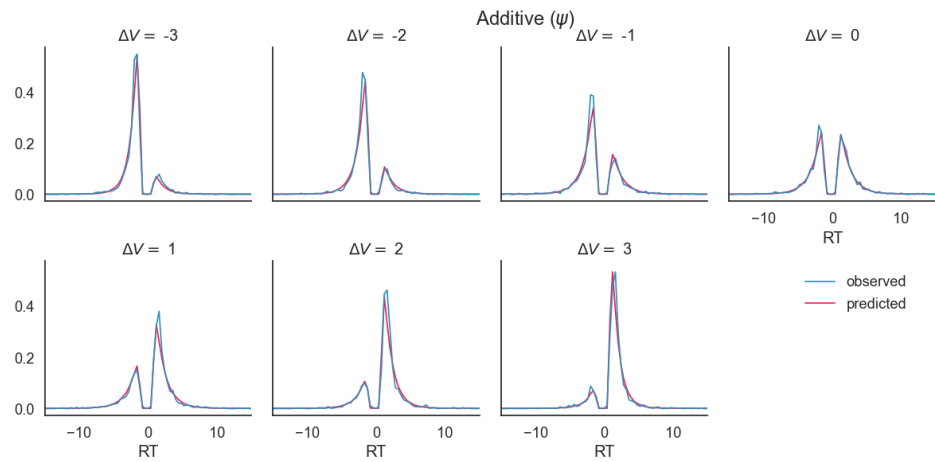


Figure S5: RT distributions (observed and predicted posteriors) from the additive DDMs; negative values = Right choices, positive values = Left choices

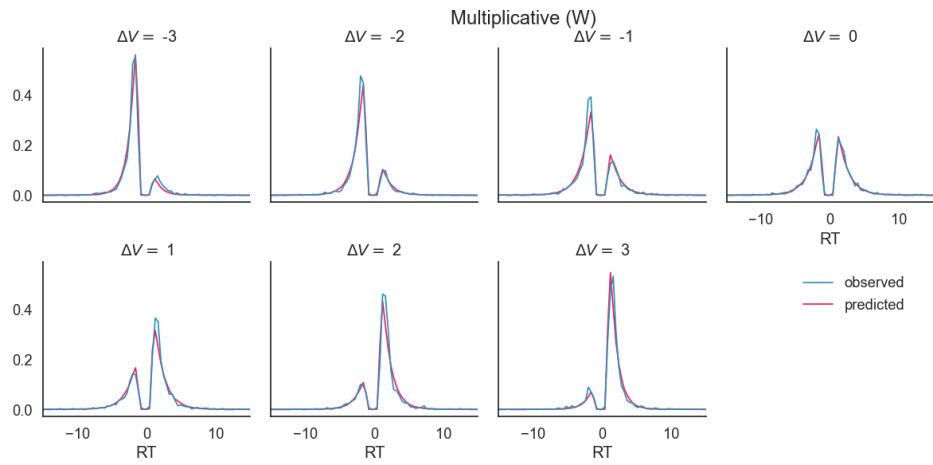
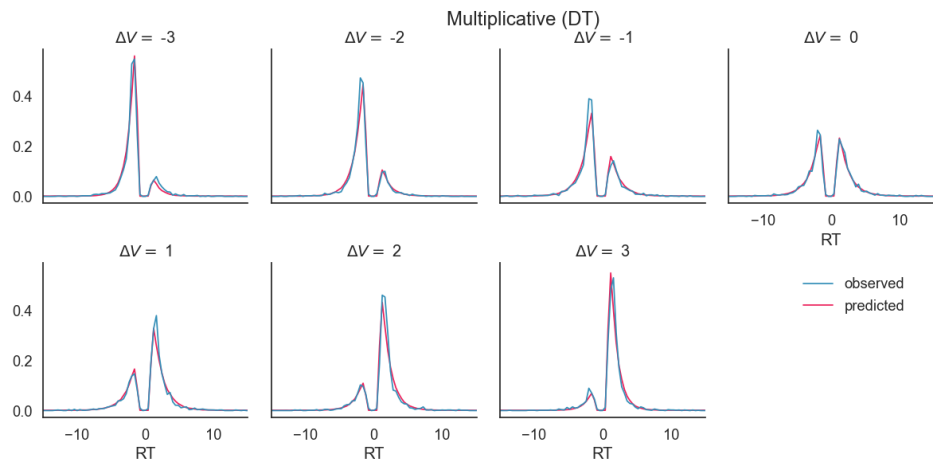
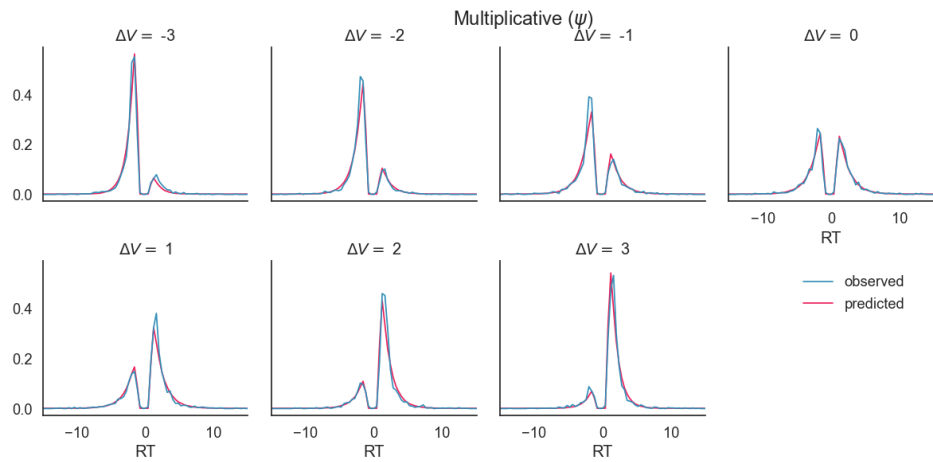


Figure S6: RT distributions (observed and predicted posteriors) from the multiplicative DDMs; negative values = Right choices, positive values = Left choices

S5 Risky choice experiment

Here, I additionally validate the scroll tracking method using another type of decision task. A risky choice experiment is arranged that is modelled after the “money-risk” task studied by Smith and Krajbich (2018) (henceforth, SK18), who use it to investigate attention and choice using eye-tracking.

S5.1 Method

In the money-risk task, subjects choose between two gambles. The gambles are lotteries, each with two outcomes and a 50% outcome probability. The outcomes vary between £0 and £5, and they are represented graphically as blue bars against a light grey background, where the height of the blue bar represents the amount of money (see Figure S7). In each pair, one of the options is always lower risk than the other, and because each outcome always has the same 50% probability of occurring, riskiness can be determined by examining the height difference between the outcomes.

The stimuli for the task were reproduced from the publicly available dataset of SK18 (<https://osf.io/g7cv6/>) and scaled to fit the outcome range of the current study. Essentially, each subject-wise series of lotteries in the SK18 money-risk dataset had an equal chance of being allocated to a subject in the current study. The pre-registered¹ study followed the same format as the consumer choice experiment in the main paper, but without the preference elicitation task (see Figures S8, S9). A general risk question (GRQ; Dohmen et al., 2011) was added at the end to model each subject’s latent risk attitude.

A total of 108 subjects participated from the Prolific subject pool (age 20–50 years, UK residents). They were paid a fixed reward of £3 and bonus payments based on their performance, which was determined by random choice of one of the choice rounds and the outcome of their chosen lottery option. The mean bonus was £3.19, and typical completion time for the study was 20 minutes. In total, 10 subjects were excluded after eliminating rounds based on pre-registered RT criteria: first, 4 subjects had 0 rounds left after excluding rounds that were quicker than 300 ms; then an additional 6 subjects were excluded because they had less than 50 rounds left after removing those rounds that were quicker than 300 ms. The final number of subjects entering the

¹Link to pre-registration: <https://doi.org/10.17605/OSF.IO/7CDBG>

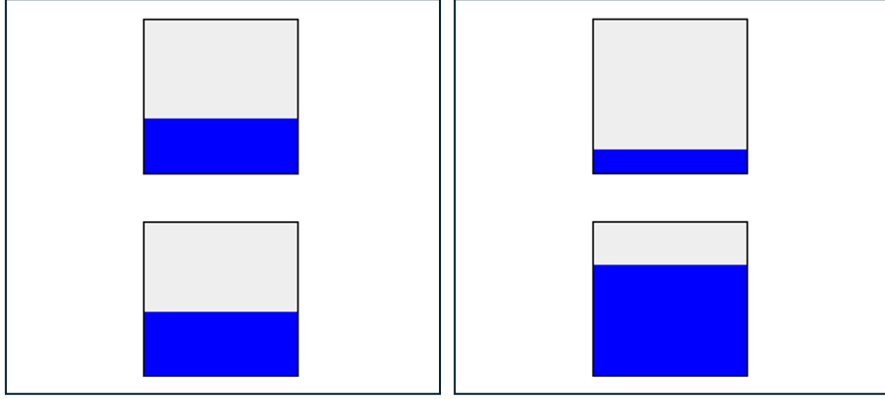


Figure S7: Example of two options in the money-risk task. The relative height of the blue bar describes the proportion of money out of £5 that is attached to the outcome. Here, the Left option is lower risk than the Right option because the difference between the bar heights is smaller on the left.

analysis is 98. All data and analysis scripts are included in the project's OSF repository.²

S5.2 Results

Utility estimation

To obtain the measurement for utility differences, the constant relative risk aversion (CRRA) utility framework (Prelec, 1998) is utilised, and the risk aversion parameter is estimated for each subject.

Assume that each outcome x is translated to utility using

$$U(x) = \frac{x^{1-\rho}}{1-\rho} \quad (\text{S1})$$

where $0 < \rho < 1$ implies risk averse and $\rho < 0$ risk seeking behaviour. The risk-aversion parameters are estimated using maximum likelihood methods; Figure S10 shows the distribution of the estimated ρ s. Given outcome pairs $(x_{L,T}, x_{L,B}), (x_{R,T}, x_{R,B})$, the expected utility difference is calculated as

$$\Delta U = E[U_L] - E[U_R] \quad \text{where} \quad E[U_i] = \frac{1}{2}(U(x_{i,T}) + U(x_{i,B})), \quad i = L, R \quad (\text{S2})$$

²Link to the file repository: <https://osf.io/25fu7/files/osfstorage>

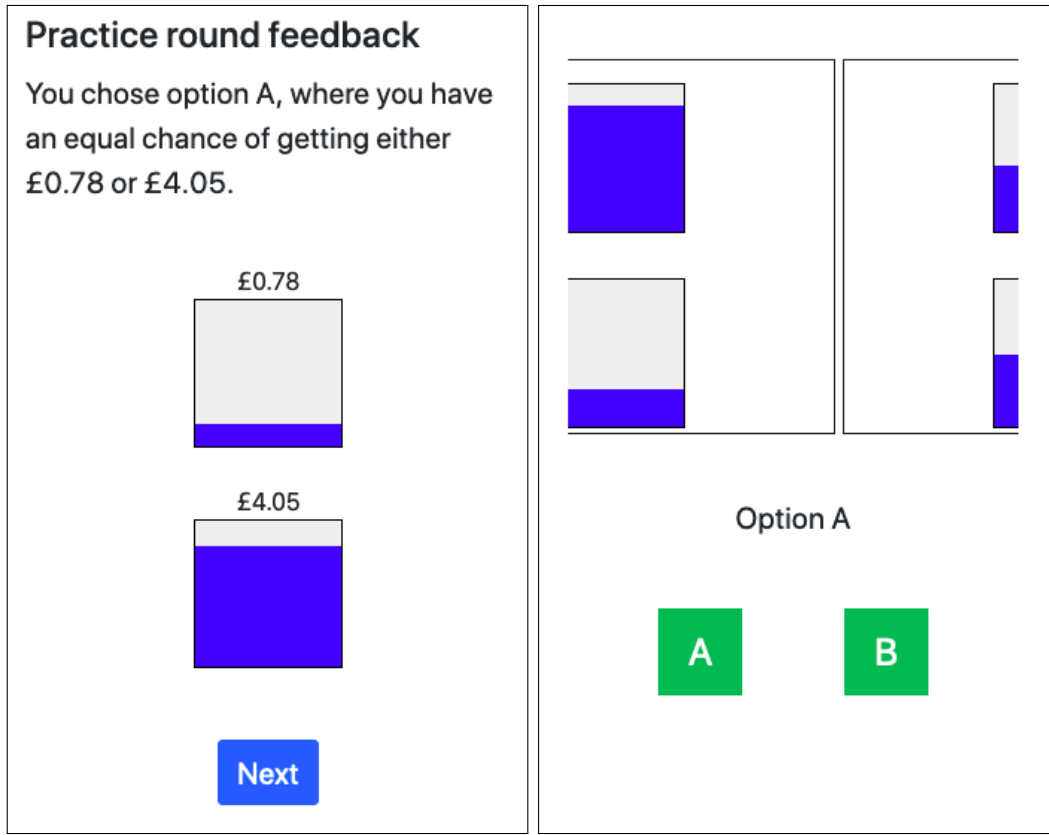


Figure S8: Screenshots from the money-risk task; the first 5 of 120 rounds were practice rounds, and the subjects saw feedback from their choices (left panel), but, in the proper decision rounds, no feedback or numerical outcome values were provided. The choices were made in a similar way to the consumer choice experiment reported in the main paper (right panel), by scrolling between them and tapping a choice button to finish the round. Each choice was a free-response and was preceded by a 1000-ms-long “loading” screen.

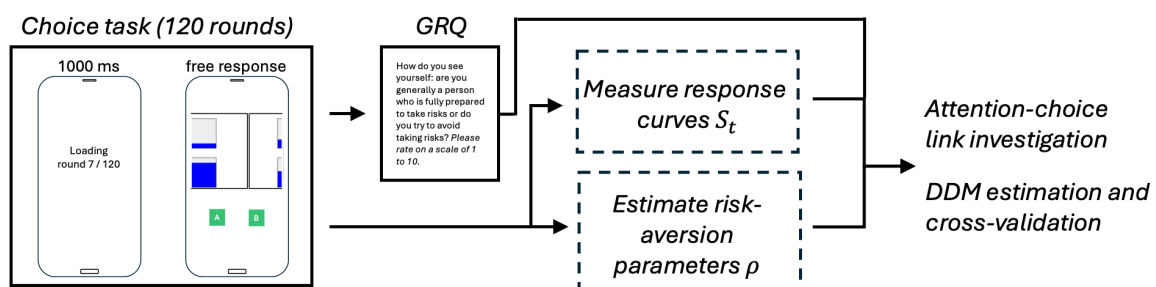


Figure S9: Experimental design for the money-risk task.

and indices T, B denote top and bottom outcomes, respectively. Each $E[U_i]$ is also scaled across participants to assume values between 0 and 1.

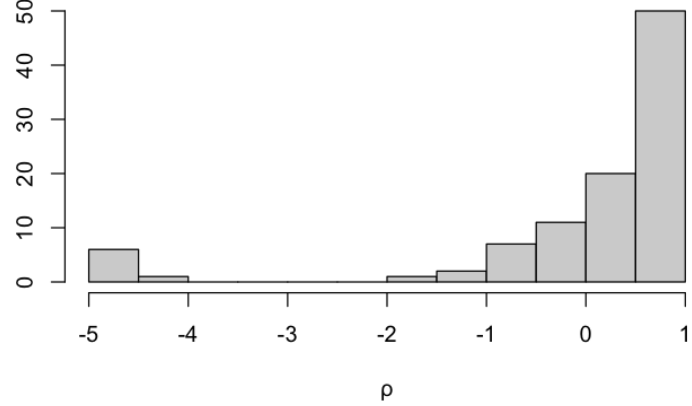


Figure S10: Histogram of ρ -values; $\rho > 0$ implies risk averse and $\rho < 0$ risk seeking behaviour

The analysis then proceeds in a similar manner to the consumer choice analysis in the main paper. First, the choice-scrolling relationship is investigated, then the subjective risk attitude parameters ρ and GRQ score are estimated from the scrolling data. Finally, the computational modelling framework is used to predict choices and response times.

Choice-scrolling link

The main analysis with the consumer choice experiment established that increased scrolling over an option increases the probability of choosing that option in a model that controls subjective value difference. Table S5 presents the same relationship for the money-risk task with subjective utility difference. The strong link between scrolling and choice can again be confirmed as evidenced by the significantly positive β_2 coefficients, although the odds ratios are smaller than with the consumer choice study (Table 1 in the main paper).

Estimating risk attitude from scrolling

Following the procedure in the main experiment with consumer choices, where subjective values are linked to the amount of scrolling, scrolling behaviour in the money-risk data is used to estimate

Table S5: Logit-GLMMs exploring the choice-scrolling link (Eq. 12 in the main paper, replacing value with utility)

	(1)	(2)	(3)
Intercept (β_0)	−0.009 [−0.11, 0.08]	−0.009 [−0.114, 0.095]	−0.009 [−0.12, 0.10]
ΔU (β_1)	0.80 [0.74, 0.87] ***	0.80 [0.74, 0.86] ***	0.82 [0.76, 0.88] ***
PRM_L^ψ (β_2)	0.61 [0.55, 0.67] ***		
PRM_L^{DT} (β_2)		0.64 [0.59, 0.70] ***	
PRM_L^W (β_2)			0.56 [0.49, 0.62] ***
RE: subject (SD)	0.48	0.48	0.48
Num. obs.	10 257	10 257	10 257

Note. RE = random effects, 95% CIs in brackets, significance: *** $p < 0.001$

the subjective parameters describing risk attitude. First, the Right option is fixed such that it is higher risk than the Left option, as follows. The outcomes in the Right option are $x_{R,T}$ and $x_{R,B}$, and the riskiness of this option can be described by $|x_{R,T} - x_{R,B}|$, i.e. the amount of money that separates the two possible outcomes that have an equal chance of being realised. The analysis is then restricted to a subset of the data such that the Left option is always the less risky one, or $|x_{R,T} - x_{R,B}| > |x_{L,T} - x_{L,B}|$, a condition that leaves us with half the observations. The hypothesis is that the amount of scrolling over the lower-risk Left option would be linked to the subject-level parameters ρ and the GRQ score. To have one observation of scrolling behaviour per subject and to be able to use linear models to investigate the predictions, the average PRM_L values are calculated for each subject in this subset of the data. The linear models are written as follows:

$$\rho \sim \beta_0 + \beta_1 \hat{\text{PRM}}_L^M \quad (\text{S3})$$

$$\text{GRQ} \sim \beta_0 + \beta_1 \hat{\text{PRM}}_L^M \quad (\text{S4})$$

where $\hat{\text{PRM}}_L^M$ is the subject-wise mean proportional response metric over all rounds where the Left option is the less risky. The results show significant relationships for Eq. S3 (for $M = \psi$, $\beta_1 = 0.82$, 95% CI = [0.56, 1.07], $p < 0.001$; for $M = DT$, $\beta_1 = 0.83$, 95% CI = [0.58, 1.08], $p < 0.001$; for $M = W$, $\beta_1 = 0.80$, 95% CI = [0.55, 1.06], $p < 0.001$), implying that the degree of relative risk aversion ρ has a positive linear relationship with the mean proportional response metrics over the less-risky option. The relationships are also significant for Eq. S4 (for $M = \psi$, $\beta_1 = -3.29$, 95%

$\text{CI} = [-5.38, -1.20]$, $p = 0.002$; for $M = DT$, $\beta_1 = -3.37$, 95% $\text{CI} = [-5.57, -1.18]$, $p = 0.003$; for $M = W$, $\beta_1 = -3.47$, 95% $\text{CI} = [-5.69, -1.25]$, $p = 0.003$), implying that the more (in average terms) the less-risky option is scrolled proportional to the riskier option, the lower is the GRQ score, or the subject's self-reported willingness to take risks in their daily life.

Stillman et al. (2020) estimate risk aversion and loss aversion parameters from a series of binary gambles and correlate them with mouse tracking area-under-the-curve measurements. They, likewise, find that subjective risk attitudes correlate with the response dynamics metric. Their correlation coefficients are in the range of $[0.26, 0.50]$ (in absolute values). Our standardised coefficient $\beta_1 = 0.55$ in the model where ρ is predicted by PRM_L^ψ (Eq. S3). Together, both studies point that response dynamics can be used to index computational risk preference measurements.

Computational modelling

Using the money-risk data, the same DDM modelling procedure is followed as in the main paper, Subsection 3.6, i.e., 4 chains are run with 4,000 draws using MCMC sampling. The only exception is the multiplicative model with dwell time, which is run using 6,000 draws and 3,000 burn-ins due to initial convergence issues. Tables S6 and S7 display the summaries from the marginal posterior distributions of the DDM parameters. The effective sample size is greater than 400 for all parameters, indicating full convergence of the chains. The β_2 coefficients, which model how drift rate responds to changes in proportional response metrics, are significantly positive but somewhat lower than in the consumer choice data reported in the main paper (Figure 6 and Table S3). For example, the β_2 coefficient for the additive DDM with ψ is 0.26 here but 0.31 with the consumer choice data. This implies a slightly weaker slope in the average rate of evidence accumulation for a unit change in proportional response metrics when the stimulus is in the risky choice rather than consumer choice format. In the money-risk data, the mean RT of 2.18 s ($SD = 1.94$ s) is lower than the mean RT in the consumer choice data (2.40 s with $SD = 1.62$ s); therefore, the subjects in the money-risk task process their choices faster than in the consumer choice study, but the relationship between the proportional amounts of scrolling and the speed of relative evidence accumulation is slightly weaker. The comparisons between observed and predicted RTs are shown in Figures S11, S12, and S13 by different binned ΔU values.

Table S6: Marginal posterior summary statistics from the basic and additive models with the money-risk data; HDI = highest density interval, ESS = effective sample size

DDM	Param	Mean	SD	HDI 2.5%	HDI 97.5%	ESS
Basic	a	1.326	0.007	1.311	1.341	21002
	t_0	0.477	0.006	0.465	0.488	22308
	z	0.509	0.004	0.501	0.517	24745
	σ_s	0.423	0.042	0.340	0.504	3158
	ν coefficients					
	intercept (β_0)	0.021	0.045	-0.069	0.110	1086
	ΔU (β_1)	0.421	0.012	0.398	0.447	30227
	Additive (ψ)	1.343	0.008	1.329	1.359	19877
	t_0	0.473	0.006	0.461	0.485	18811
	z	0.510	0.004	0.502	0.518	23819
	σ_s	0.489	0.044	0.402	0.574	3176
	ν coefficients					
	intercept (β_0)	0.022	0.050	-0.076	0.120	827
	ΔU (β_1)	0.398	0.012	0.374	0.422	22440
	ΔPRM (β_2)	0.260	0.011	0.238	0.282	21192
Additive (DT)	a	1.345	0.008	1.330	1.360	18110
	t_0	0.473	0.006	0.461	0.485	17576
	z	0.510	0.004	0.502	0.518	19703
	σ_s	0.493	0.044	0.408	0.581	3304
	ν coefficients					
	intercept (β_0)	0.017	0.050	-0.084	0.111	742
	ΔU (β_1)	0.393	0.012	0.370	0.417	23961
	ΔPRM (β_2)	0.280	0.012	0.258	0.303	19470
	Additive (W)	1.343	0.008	1.327	1.357	14381
	t_0	0.474	0.006	0.462	0.486	14527
	z	0.510	0.004	0.502	0.518	21399
	σ_s	0.517	0.045	0.431	0.607	3073
	ν coefficients					
	intercept (β_0)	0.021	0.052	-0.078	0.127	637
	ΔU (β_1)	0.399	0.012	0.376	0.424	18737
	ΔPRM (β_2)	0.295	0.014	0.268	0.323	15106

Table S7: Marginal posterior summary statistics from the multiplicative models with the money-risk data; The coefficients are denoted $C_1 \equiv \text{PRM}_L U_L - \text{PRM}_R U_R$, $C_2 \equiv \text{PRM}_R U_L - \text{PRM}_L U_R$; HDI = highest density interval, ESS = effective sample size

DDM	Parameter	Mean	SD	HDI 2.5%	HDI 97.5%	ESS
Multiplicative (ψ)	a	1.345	0.008	1.329	1.360	17017
	t_0	0.472	0.006	0.460	0.484	15952
	z	0.510	0.004	0.502	0.518	22169
	σ_s	0.491	0.045	0.407	0.581	2661
	ν coefficients					
	intercept (γ_0)	0.019	0.051	-0.087	0.116	594
	C_1 (γ_1)	1.007	0.027	0.954	1.060	11020
	C_2 (γ_2)	0.716	0.026	0.664	0.769	10887
Multiplicative (DT)	a	1.347	0.008	1.332	1.362	23701
	t_0	0.472	0.006	0.460	0.484	24213
	z	0.510	0.004	0.502	0.517	26191
	σ_s	0.493	0.044	0.405	0.579	4372
	ν coefficients					
	intercept (γ_0)	0.021	0.051	-0.082	0.117	1060
	C_1 (γ_1)	0.981	0.026	0.931	1.033	15573
	C_2 (γ_2)	0.674	0.025	0.625	0.725	15832
Multiplicative (W)	a	1.342	0.008	1.327	1.357	14979
	t_0	0.474	0.006	0.461	0.486	14753
	z	0.510	0.004	0.502	0.517	20730
	σ_s	0.505	0.045	0.418	0.593	3091
	ν coefficients					
	intercept (γ_0)	0.020	0.052	-0.081	0.121	673
	C_1 (γ_1)	0.904	0.024	0.857	0.949	11749
	C_2 (γ_2)	0.607	0.023	0.562	0.653	11276

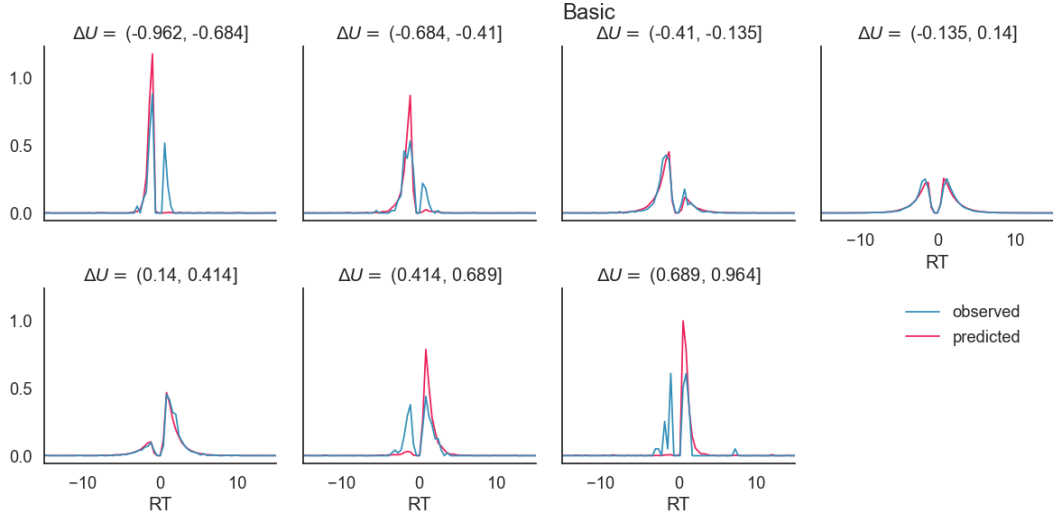


Figure S11: Money-risk RT distributions (observed and predicted posteriors) from the basic DDM; negative values = Right choices, positive values = Left choices

To compare the predictive ability of the different DDMs in the money-risk task, again the same hold-out evaluation procedure is followed as in the main paper (Subsection 3.6). Data from odd-numbered rounds is used to estimate the additive and multiplicative DDMs and derive posterior predictive distributions of choices for even-numbered rounds. Then, a set of predicted choices is compared to the real choices on even rounds, and the share of correctly predicted choices is calculated for each draw in each chain. This results in $4 \text{ chains} \times 4,000 \text{ draws} = 16,000$ correctness scores, which are summarised for different models in Table S8.

Table S8: Predictive correctness of DDMs estimated on odd rounds; score = mean % of even round choices predicted correctly

DDM	Score
Basic	56.9%
Additive (ψ)	59.3%
Additive (DT)	59.5%
Additive (W)	58.8%
Multiplicative (ψ)	59.3%
Multiplicative (DT)	59.6%
Multiplicative (W)	58.7%

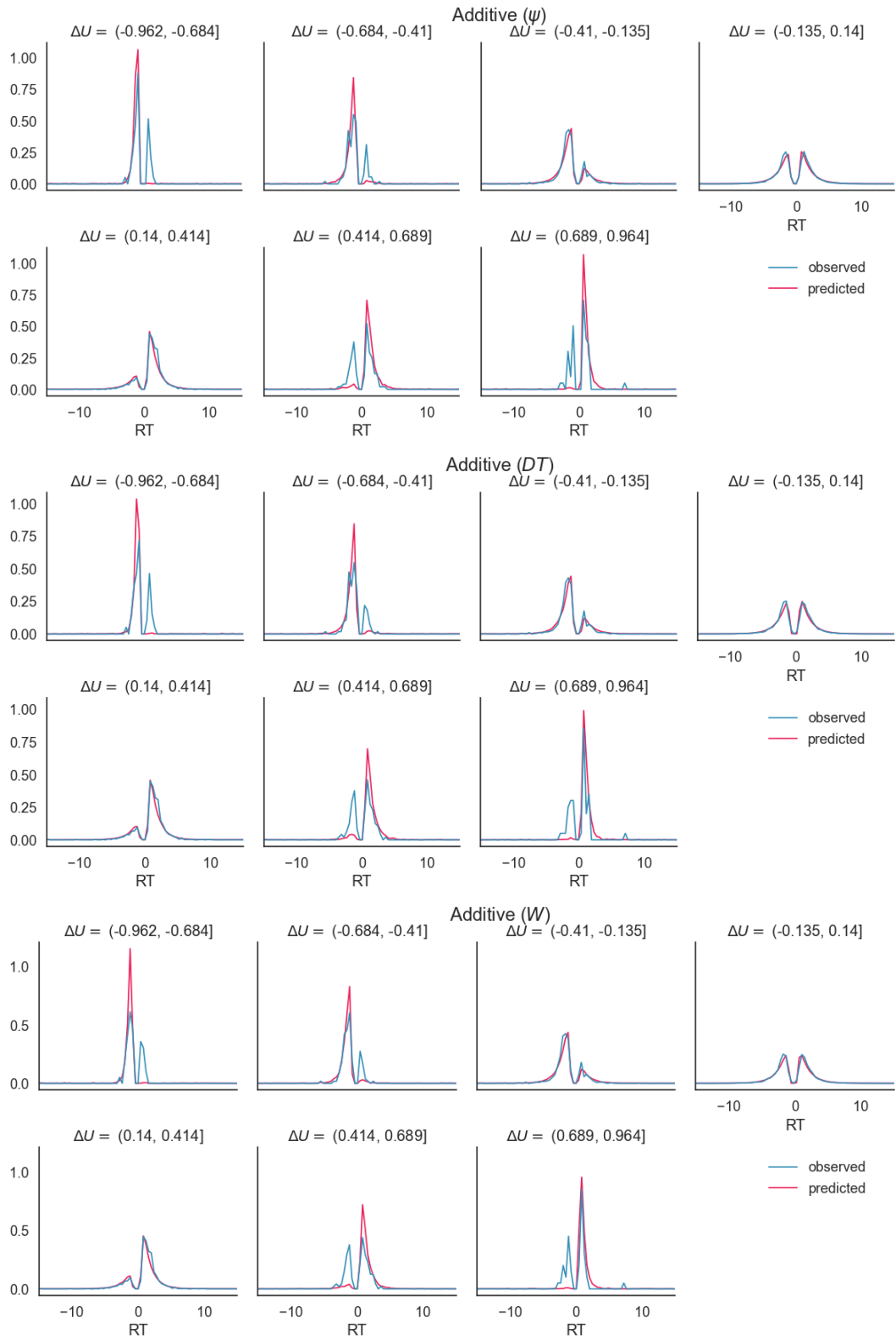


Figure S12: Money-risk RT distributions (observed and predicted posteriors) from the additive DDMs; negative values = Right choices, positive values = Left choices

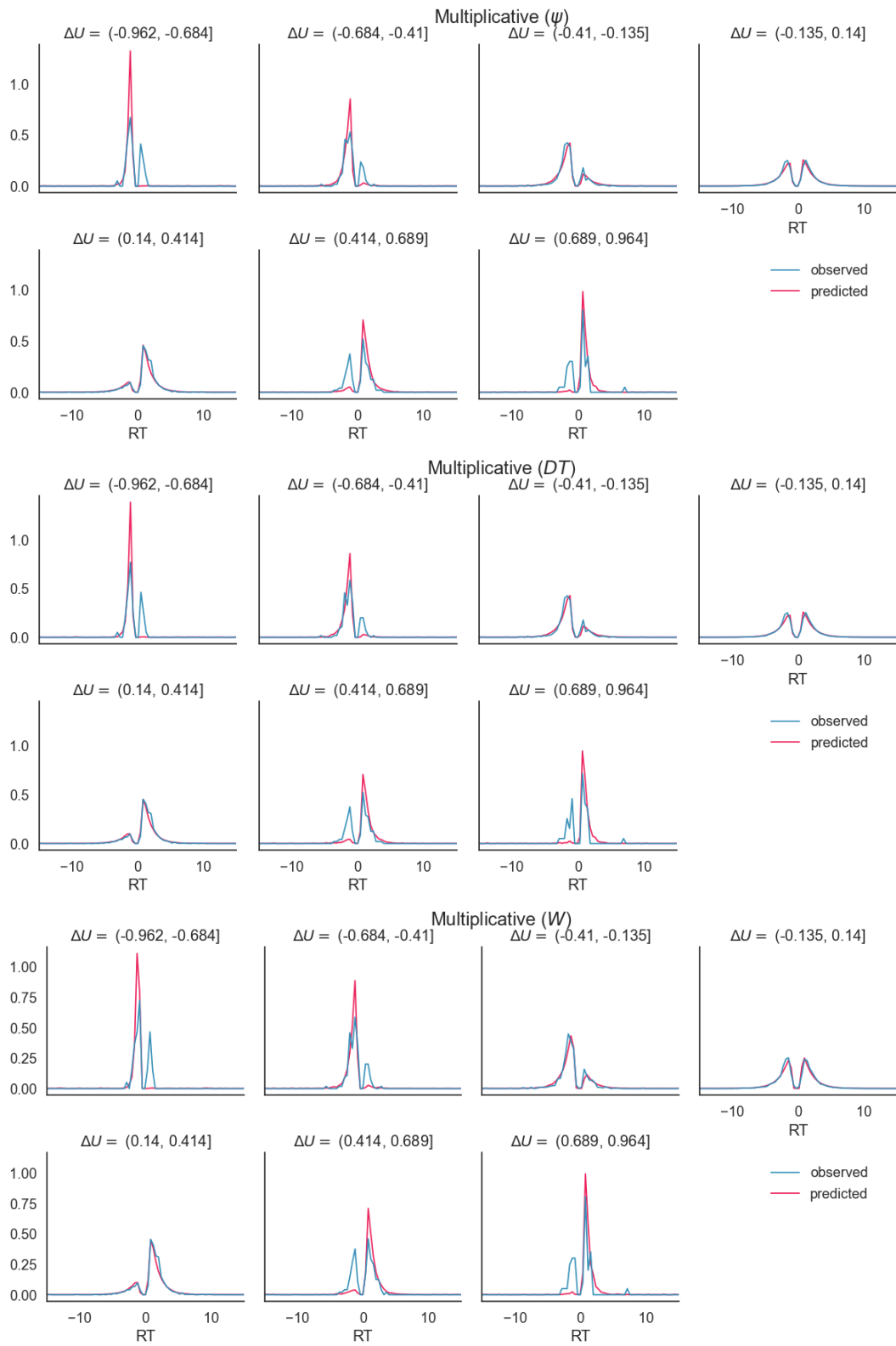


Figure S13: Money-risk RT distributions (observed and predicted posteriors) from the multiplicative DDMs; negative values = Right choices, positive values = Left choices

S5.3 Re-analysis of the SK18 data

The SK18 dataset includes region-of-interest dwell times, and this allows the proportional dwell time metrics, PRM_L^{DT} , to be calculated and compared to the results from the scroll tracking metrics presented in the previous section (Table S5). To prepare the comparisons, two re-calculations are performed from the SK18 data: (1) The PRM_L^{DT} metrics are calculated for each choice based on the left/right dwell time data provided in SK18 dataset, and (2) the ρ_s (CRRA utilities, Eq. S1) and expected utility differences ΔU (Eq. S2) are calculated using the utility estimation procedure described in the previous section, based on the choice and lottery value data in the SK18 dataset. Then, the subset of rounds 1–120 from the SK18 data is used to make the re-analysis comparable with the scroll tracking data, which contained 120 rounds (SK18 originally collected 200 rounds from each of the 36 subjects). Table S9 shows the results of a logistic GLMM of the re-analysis, which is also presented in the main paper, Figure 7 and can be directly compared to Table S5. The β_2 coefficient in the re-analysed SK18 data (which is restricted to rounds 1–120) is higher (0.97) than in the scroll tracking data ($\beta_2(DT) = 0.64$), which implies that choice probability is more sensitive to response metrics calculated from eye-tracking data than from scroll tracking data.

Table S9: Logistic GLMM for SK18 eye data (Eq. 12 in the main paper)

Intercept (β_0)	0.097 [−0.013, 0.21]
ΔU (β_1)	0.79 [0.70, 0.88] ***
PRM_L^{DT} (β_2)	0.97 [0.88, 1.06] ***
RE: subject (SD)	0.25
Num. obs.	3974

Note. RE = random effects, 95% CIs in brackets, significance: *** $p < 0.001$

Finally, cross-validation is used to predict even round choices using DDMs constructed from odd rounds in the SK18 data. The predictive correctness scores are reported in the main paper.

S6 Comparison of response metrics between studies

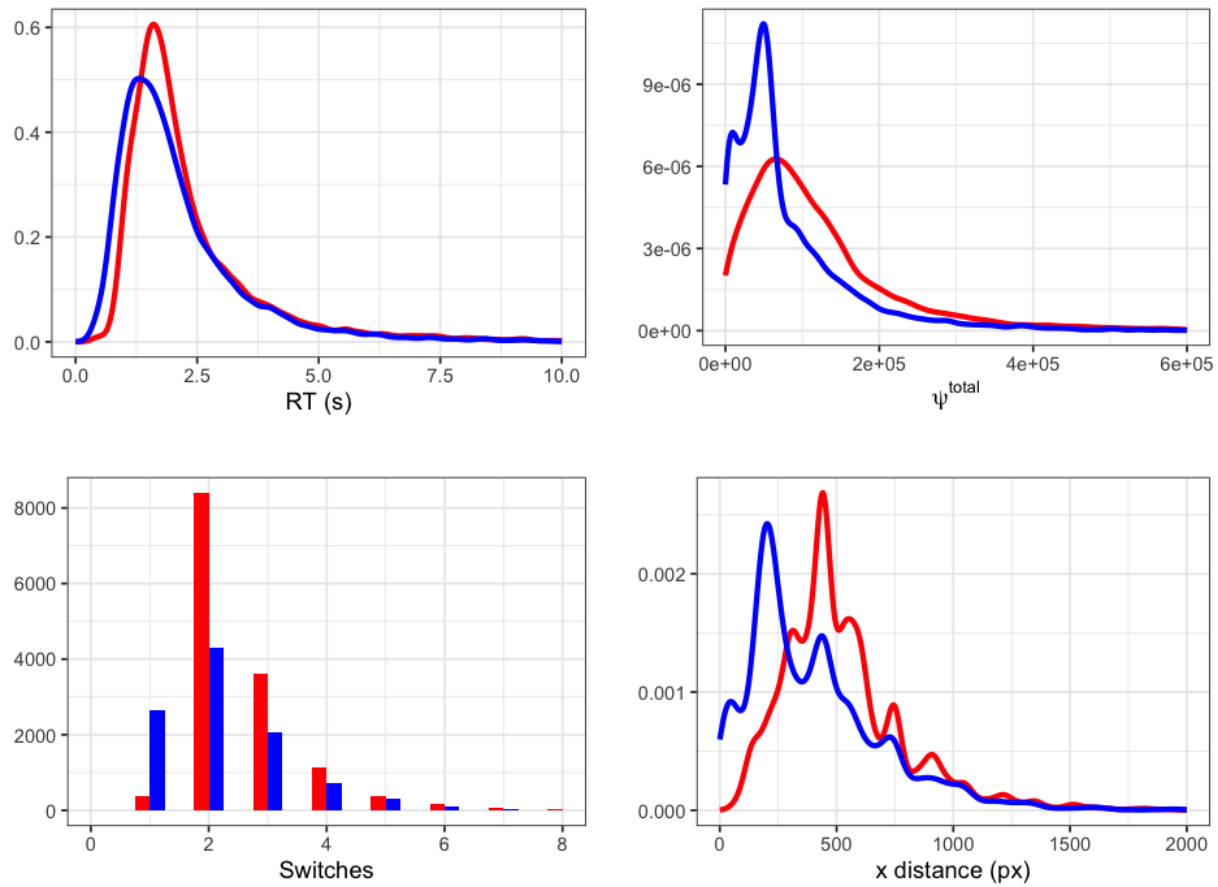


Figure S14: Comparison of aggregate response metric distributions between studies. Red = consumer choice, Blue = money-risk task.

References

Cavanagh, J. F., Wiecki, T. V., Kochar, A., and Frank, M. J. (2014). Eye tracking and pupillometry are indicators of dissociable latent decision processes. *Journal of Experimental Psychology: General*, 143(4):1476.

Dohmen, T., Falk, A., Huffman, D., Sunde, U., Schupp, J., and Wagner, G. G. (2011). Individual risk attitudes: Measurement, determinants, and behavioral consequences. *Journal of the European Economic Association*, 9(3):522–550.

Prelec, D. (1998). The probability weighting function. *Econometrica*, pages 497–527.

Smith, S. M. and Krajbich, I. (2018). Attention and choice across domains. *Journal of Experimental Psychology: General*, 147(12):1810.

Stillman, P. E., Krajbich, I., and Ferguson, M. J. (2020). Using dynamic monitoring of choices to predict and understand risk preferences. *Proceedings of the National Academy of Sciences*, 117(50):31738–31747.